ENERGY DISSIPATION IN HELICON PLASMA AT THE NEAR FIELD OF AN ANTENNA

V. Olshansky

National Science Center "Kharkov Institute of Physics and Technology", Institute of Plasma Physics, Kharkiv, Ukraine

The results of a computer simulation of energy dissipation in helicon plasma at near field of an antenna are presented. Results are reported for a double-half-turn antenna, and comparison is made to a double-saddle-coil antenna which demonstrates the distinct inductive and helicon-wave modes. The computer simulation revealed a significant wave-particle interaction in the near-field of the antenna that is less than half wavelengths from the antenna. Namely, in addition to the ohmic heating from the currents induced by the helicon wave, electrons can become trapped in the traveling helicon wave via the resonance condition.

PACS: 52.50.Dg; 52.50.Qt ;52.65.-y; 52.80.Pi

INTRODUCTION

As well known the helicon waves propagate in magnetized plasmas for frequencies between the ion and electron cyclotron frequencies and have been found to be very effective in creating high plasma densities both in linear and toroidal systems. The partial ionization level in such devices can be large enough. Nevertheless, the electron distribution function can be strongly non-equilibrium and can differ considerably from the Maxwellian one. It affects the discharge properties and leads to the non-uniform and nonlinear power absorption. Hence, for adequate simulation of the energy dissipation in helicon plasma the kinetic plasma description should be used. One of the important factors that should be taken in account in a computer simulation of plasma discharges with moderate partial ionization is the electron collisions and other collisions that essentially affect thermal motion of plasma particles. There are several approaches to deal with collisions in a plasma discharge. We use the approach that utilizes Monte Carlo method for simulation collisions between plasma particles and neutrals in conjunction with the particle-mesh algorithm [1, 2].

It is so called "Particle-in-cell/Monte Carlo Collisions" (PM/MCC) method that no assumption requires for particle distribution function on energy. It allows using realistic differential cross sections during collisions simulation. This method is most effective for the kinetic simulation of plasma discharges of low pressure, since in such plasma the charged particles collisions with neutrals are rare enough, and electrons free path is comparable with characteristic system length.

This paper presents the results of computer simulation of energy dissipation in helicon plasma at near field of an antenna. Results are reported for a double-half-turn antenna, and comparison is made to a double-saddle-coil antenna which demonstrates the distinct inductive and helicon-wave modes.The computer simulation revealed a significant wave-particle interaction in the near-field of the antenna that is less than half wavelengths from the antenna. Namely, in addition to the ohmic heating from the currents induced by the helicon wave, electrons can become trapped in the traveling helicon wave via the resonance condition given by $\omega - k_p v_p = 0$, where k_p and v_p are the wave vector and electron velocity, respectively, parallel to the axial magnetic field. Considerable attention has been paid to the ''helicon jump'' above which the plasma was assumed to be operating with helicon wave heating. A large increase in plasma density (n_0), coupled with decreases in plasma potential (V_p), and the electron temperature (T_e), have been computed across the jump, and a fundamental change in the EM-mode are shown.

1. MODEL GEOMETRY

Geometry of the model corresponds to the model of standard helicon ion source. It consists from cylindrical resonator with perfect conducting walls, plasma column which confined in cylindrical dielectric chamber (a vessel from quartz or glass). Between the outward chamber surface and metal wall of the resonator there is vacuum gap. Plasma resides in the external stationary magnetic field. RF antenna, which excites the electromagnetic field, can be placed inward or outward relative to the plasma.

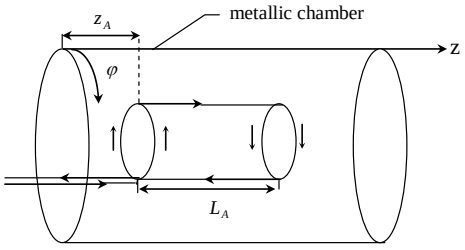

Fig. 1. The scheme of the antenna placement

The antenna placement scheme is shown in Fig. 1. Since the antenna is situated in the metallic resonator, then the Fourier spectra of the current and excited fields are discrete with respect to axial coordinate. However, if one assumes the antenna conductors infinite thin, the spectrum over axial coordinate is found infinite too (the amplitudes of Fourier harmonics not decrease with increase of the longitudinal wave number). Therefore in the computer model the finite dimensions of the antenna conductors are taken into account. Then the harmonics amplitudes decrease with increase of the wave number and Fourier series is convergent (Fig. 2). Analytically antenna is given by the current that flows in antenna conductors of finite dimensions h placed on cylindrical surface of the radius r_a (see Fig. 1).

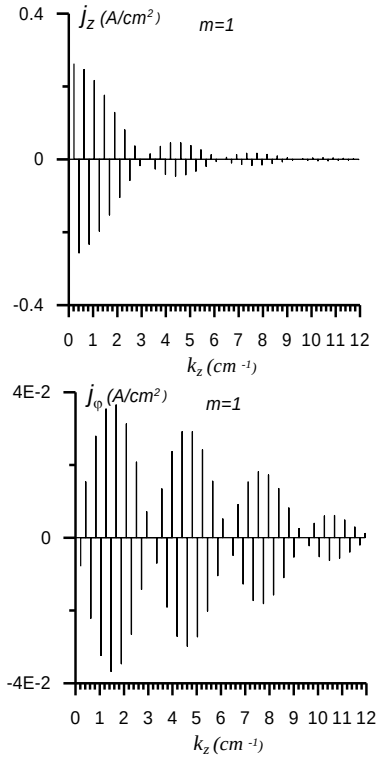

Fig. 2. Axial and azimuthal spectra of the antenna Nagoya type III with finite dimensions of conductors taking into account (L_a =14 cm, R_a =2 cm, L_{ch} =15 cm, Z_a =0 cm, I_0 =100 A, mode m=+1)

2. ELECTROMAGNETIC FIELD

Electromagnetic module solves Maxwell's equations

$$\mathrm{rot}\mathbf{B} = \frac{4\pi}{c}\mathbf{j} + \frac{1}{c}\frac{\partial \mathbf{E}}{\partial t},\ \mathrm{rot}\mathbf{E} = -\frac{1}{c}\frac{\partial \mathbf{B}}{\partial t},$$
$$\mathrm{div}\mathbf{E} = 4\pi\rho,\ \mathrm{div}\mathbf{B} = 0.$$

The current and charge densities in the Maxwell's equations are defined by the distribution functions of electrons and ions by formulae $\mathbf{j} = \sum_{i,e} q_{i,e} \int f_{i,e}\mathbf{v}\mathrm{d}\mathbf{v}$, $\rho = \sum_{i,e} q_{i,e} \int f_{i,e}\mathrm{d}\mathbf{v}$, where the indexes i and e denote the kind of the particles, i.e. ions and electrons respectively; $f_{i,e}$ are distribution function of the particles; $q_{i,e}$ are the charges; **E** and **B** are the electric and magnetic fields. The Maxwell's equations are solved in Euler variables. The charge and current densities, necessary for their solution, are computed through the velocities and coordinates of the separate particles

$$\rho(\mathbf{r},t) = \sum_{j=1}^{J} q_j R\left(\mathbf{r},\mathbf{r}_j(t)\right),\ \mathbf{j}(\mathbf{r},t) = \sum_{j=1}^{J} q_j \mathbf{v}_j(t) R\left(\mathbf{r},\mathbf{r}_j(t)\right).$$

For the electric and magnetic fields computation proposed in [9] computation scheme is used.

3. SIMULATION PARAMETERS

The dispersion relation for the helicon wave is [3]

$$D(\omega,k) \equiv \frac{k^2c^2}{\omega^2} - \frac{\omega_{pe}^2}{\omega\left(\omega_{ce}\left(k_\parallel/k\right) - \omega\gamma_e\right)},$$

where $k^2 = k_\parallel^2 + k_\perp^2$ is wave number, $\gamma_e = 1 + i\left(\nu_e/\omega\right)$. For the natural modes of the plasma we have $D = 0$. This dispersion relation is for planar geometry. For cylindrical geometry one can use the following definition for the transverse wave number $k_\perp = \alpha(m,n)/a$, where $\alpha(m,n)$ is the argument giving the nth zero of the m-th order Bessel function and a is a cylinder radius. Note, for any combination of plasma parameters there exists $k_\parallel$, which satisfies $D = 0$, and therefore a helicon wave can exist for all densities. One can see from dispersion relation that the limit $k_\parallel = k_\perp$ corresponds to low plasma density, and the $k_\parallel = k_\perp$ limit corresponds to high plasma density. One can distinguish them by setting condition $n = n_0$ for which $k_\parallel = k_\perp$ for the $m = 1$ helicon mode. Then, $k = \sqrt{2}k_\perp$, and $k_\parallel = k_\perp \approx 2.5/a$ [4]. Choosing the typical experimental parameters a=5 cm, f=13.56 MHz, and B_0=200 G we have $n_0 \approx 4\times10^{12}$ cm^{-3}.

4. PARTICLES COLLISIONS ACCOUNTING

During the time Δt the collision probability of the particle that moves with the velocity $v(t_n)$ is calculated by the formula $P_i = 1 - \exp\left[-n_g(\vec{r})\sigma_T(E_i)v_i\Delta t\right]$, where $n_g(\vec{r})$ is the target particles density, and the total cross section $\sigma_T(E_i)$ depends on the particle energy E_i, and it is defined as a sum over all collision processes

$$\sigma_T(E_i) = \sum\nolimits_j \sigma_j(E_i).$$

For the particles collisions accounting we use null collision method [5]. For this we introduce the fictitious collision $\nu_{\max} = \max_{\vec{r}}\left(n_g(\vec{r})\right)\max_{E}\left(\sigma_T(E)v\right)$, and total probability of the collision which not depends on energy and coordinates of the particle $P_T = 1 - \exp\left[-\nu_{\max}\Delta t\right]$.

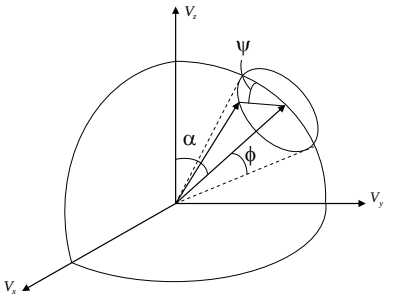

Fig. 3. Velocity vector scattering; α is the angle between velocity and the axis V_z before collision, ϕ is the scattering angle, the angle ψ sets the orientation of the scattering plane in the scattering cone

Further $N_c = P_T N$ random particles are choosing from the total particles list and for them only the collision process is calculated. In Fig. 3 the scheme of the velocity vector scattering and the angles which correspond to velocity vector direction after collision are shown. For the electron-ion elastic collisions the angle ψ is given by the random number from the interval [0.2π]. Distribution of the scattering angle ϕ is given in correspondence to the Spitzer formula for small angle scattering [6].

$$P(\phi)d\phi = \left(\phi d\phi / \left\langle \phi^2 \right\rangle_{\Delta t}\right)\exp\left[-\phi^2 / 2\left\langle \phi^2 \right\rangle_{\Delta t}\right],$$

where $\left\langle \phi^2 \right\rangle = (3/2)\omega_p \left(\ln\Lambda / \Lambda\right)$. The distribution function reversal gives

$$\phi(R) = F^{-1}(R) = \left[-2\left\langle \phi^2 \right\rangle \Delta t \ln(1-R)\right]^{1/2},$$

where R is a random number from the [0,1] interval. The empirical formula for the elastic scattering between electrons and argon atoms is presented in [7]

$$\frac{\sigma(E,\phi)}{\sigma(E)} = \frac{E}{4\pi\left[1+E\sin^2(\phi/2)\right]\ln(1+E)}.$$

Using this formula we write the distribution function

$$R = F(\phi) = \int_0^{\phi} \sigma(E,\phi')\sin\phi' d\phi' \Big/ \int_0^{\pi} \sigma(E,\phi')\sin\phi' d\phi'.$$

This function reversal gives the scattering angle cosine distribution $\cos\phi = \left(2+E-2(1+E)^R\right)/E$. As a result of the collision the partial electron energy loss can be calculated by the formula $\Delta E = (2m/M)(1-\cos\phi)E$.

Consider the process of the impact ionization. Energy balance for impact ionization is $E_{sc} + E_{cr} = E_i - E_{iz}$, where E_{sc} is the scattered electron energy, E_{cr} is the born electron energy, E_i is the electron energy before collision with neutral atom and E_{iz} is the ionization energy. For the ionization process with no high energy E_i differential cross section is given in the following form [8]

$$S(E_i, E_{sc}) = \frac{\sigma_{iz}(E_1)B(E_i)}{\arctan\left\{\left[E_i - E_{iz}\right]/\left[2B(E_i)\right]\right\}\left[E_{sc}^2 + B^2(E_i)\right]}.$$

Here $B(E_i)$ is the function which is specific for the different gases. In particular, B; 10 eV for Argon. Introducing the distribution function

$$R = \int_0^{E_{sc}} S(E_i, E'_{sc})dE'_{sc} \Big/ \int_0^{(E_i - E_{iz})/2} S(E_i, E'_{sc})dE'_{sc},$$

and reversing it we obtain energy distribution of the scattered electron

$$E_{sc} = B(E_i)\tan\left[R \cdot \arctan\left((E_i - E_{iz})/(2B(E_i))\right)\right].$$

5. SIMULATION RESULTS

The computed axial wave profiles at the frequencies f = 13.56 and 27.12 MHz are shown in Figs. 4 and 5, respectively. As one can see in Fig. 4,a, the wave profile at smaller magnetic field ($B \sim 100$ G) is independent of the plasma density. At higher density ($n = 4\cdot 10^{12} cm^{-3}$) and higher magnetic field ($B \sim 200$), it becomes a more short wavelength mode as shown in Fig. 4,b. The wavelength at the frequency $f = 27.12$ MHz has density dependence at $B \sim 100$ G and density independence at $B \sim 200$ G as shown in Figs. 5,a and 5,b. As one can see two types of waves exist here. The transverse wave number $k_{\perp}$ can be computed from the wave field structure. For the calculation of the dispersion relation the axially averaged density and computed transverse wave number is used. The helicon wave dispersion relation somewhat deviates from the simulation data, but this may be the result of the uniform plasma assumption in the theoretical formula.

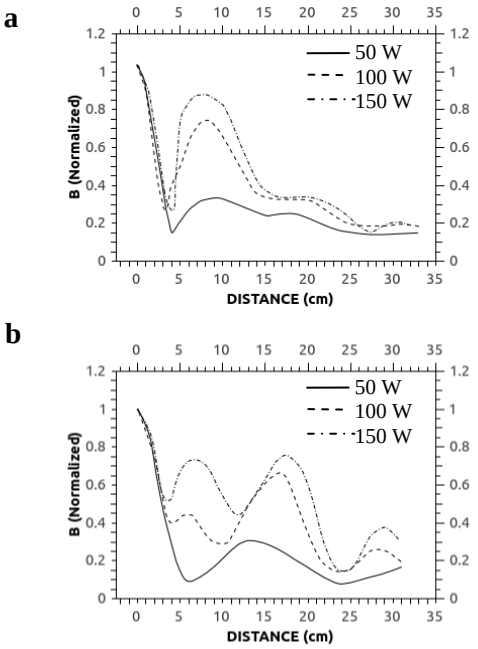

Fig. 4. Axial profile of the wave with frequency f= 13.56 MHz (distance is accounted from the antenna)

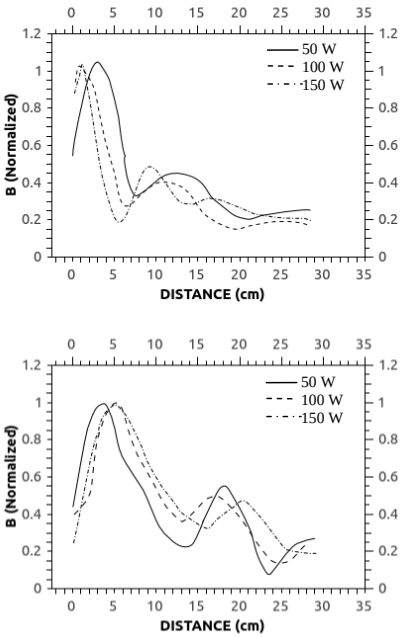

Fig. 5. Axial profile of the wave with frequency f=27.12 MHz (distance is accounted from the antenna)

By applying an external magnetic field with different strength a plasma mode transition from E to H discharge mode is observed. Once the plasma reaches the H discharge mode, inductive coupling becomes the dominant plasma heating mechanism. Even though the external magnetic field is switched off, plasma can be sustained by the inductively coupled discharge mode (H mode). This H mode is characterized by a localized high density. Then the W wave propagation helicon mode is switched on by the external magnetic field and plasma density jump is

observed. The azimuthally symmetric ($m=0$ mode) wave at the first harmonic at becomes a helicon wave at high density ($n \sim 2.2 \cdot 10^{12} cm^{-3}$) and high magnetic field ($\omega_c / \omega > 30$).

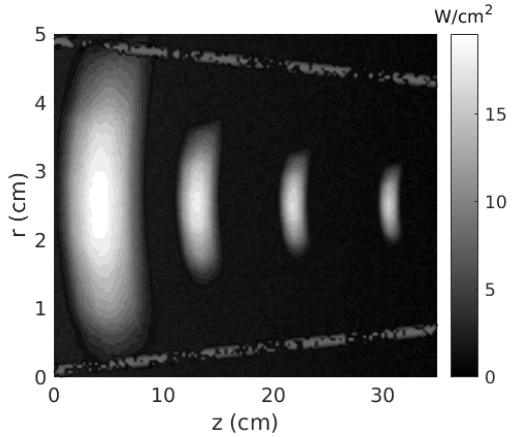

Fig. 6. Absorbed power density

The RF power absorption density calculated for $f = 13.56$ MHz is shown in Fig. 6. Most of the power is absorbed by the electrons in the bulk of the plasma, with 75 % of the total power absorbed at r<4.5 *cm* and z<35 *cm*. The plot of absorbed power density shows a quasi-periodic structure along z axis and an additional narrow elongated structure that appears under the antenna. The quasi-periodic peaks of the power absorption in the axial direction can be produced by the RLH eigenmode [10], because the ideally conducting walls of the source form a cavity for the the eigenmodes in the axial direction. As a result, the plot Fig. 6 shows a sequence of peaks in the z direction. The collisional power dissipation in this mode is associated with the axial component of the electron current. This component is considerably increases in the regions with large radial density gradient. In this case a Hall current that has a radial component is produced. In the region with large radial density gradient, the radial Hall current should be supplemented with strong longitudinal current to keep the divergence free of the total plasma current and preclude charge separation. The enhancement of the axial electron current is the cause of radial localization of the RF power absorption in the region with strong radial gradient. The narrow elongated structure in the power absorption in Fig. 6 is associated with excitation of electrostatic TG [11] waves. The TG waves are excited due to mode coupling, which is most pronounced at the plasma edge, where the radial Hall current from the RLH wave produces a surface charge.

REFERENCES

1. Y. Weng, M.J. Kushner // *Phys. Rev. A.* 1990, v. 42, p. 6192.
2. R. Kinder, M. J. Kushner // *J. Appl. Phys.* 2001, v. 90, p. 3699.
3. K.P. Shamrai. Theory of radio-frequency power absorption in helicon plasmas. Manuscript // *Thesis.* V.N. Karazin Kharkiv National University, Kharkov, 2008.
4. A.M. Lieberman, A.J. Lichtenberg. *Principles of Plasma Discharges and Materials Processing* / Second ed. "John Wiley & Sons", 2005.
5. V. Vahedi, M. Surendra. Monte-Carlo Collision Model for Particle-in-Cell method: Application to Argon and Oxygen Discharges // *Comp. Phys. Comm*. 1995, v. 87, p. 179-198.
6. L. Spitzer // *Jr. Physics of Fully Ionized Gases* / 2nd ed., New York: "Wiley-Interscience", 1962.
7. M. Surendra, D. B. Graves, I.J. Morey // *Appl. Phys. Lett.* 1990, v. 56, p. 1022-4.
8. C.B. Opal, W.K. Peterson, E.C. Beaty // *J. Chem. Phys*. 1971, v. 55, p. 4100.
9. A.B. Langdon, B.F. Lasinski. Electromagnetic and relativistic plasma simulation models // *Meth. Comput. Phys.* 1976, v.16, p. 327-366.
10. B.N. Breizman, A.V. Arefiev. Radially Localized Helicon Modes in Nonuniform Plasma // *Phys. Rev. Lett*. 2000, v. 84, № 17, p. 3863-3866.
11. K.P. Shamrai, V.B Taranov. Volume and surface rf power absorption in a helicon plasma source // *Plasma Sources Sci. Technol*. 1996, v. 5, p. 474-491.

Article received 12.09.2018

ПОГЛОЩЕНИЕ ЭНЕРГИИ В ГЕЛИКОННОЙ ПЛАЗМЕ В БЛИЖНЕМ ПОЛЕ АНТЕННЫ

В.В. Ольшанский

Представлены результаты компьютерного моделирования диссипации энергии в геликонной плазме в ближнем поле антенны. Результаты даны для «double-half-turn»-антенны и сравниваются с «double-saddle-coil»-антенной, которая демонстрирует различные индуктивные и геликонные волновые моды. Компьютерное моделирование обнаруживает существенное взаимодействие волна-частица в ближнем поле антенны на расстоянии менее половины длины волны от антенны. В дополнение к омическому нагреву током, индуцированным геликонной волной, электроны могут захватываться распространяющейся геликонной волной при наличии резонанса.

ПОГЛИНАННЯ ЕНЕРГІЇ В ГЕЛІКОННІЙ ПЛАЗМІ В БЛИЖНЬОМУ ПОЛІ АНТЕНИ

В.В. Ольшанський

Представлено результати комп'ютерного моделювання дисипації енергії в геліконній плазмі в ближньому полі антени. Результати наведені для «double-half-turn»-антени та порівнюються з «double-saddle-coil»-антеною, яка демонструє різні індуктивні та геліконні хвильові моди. Комп'ютерне моделювання виявляє суттєву взаємодію хвиля-частинка в ближньому полі антени на відстані менш ніж половина довжини хвилі від антени. В додаток до омічного нагрівання струмом, що індукується геліконною хвилею, електрони можуть бути захопленими геліконною хвилею, що розповсюджується, при наявності резонансу.